

ESTIMATION OF OPTO-MECHANICAL PARAMETERS FOR CALIBRATION OF LASER SCANNERS

Qing FU^a, Hongchao FAN^{b,*}, Aloysius WEHR^c, Uwe STILLA^b

^aInstitute of Geodesy and Geophysics, Vienna university of technology, Gusshausstr.27-29/E128-3, A- 1040 Vienna, Austria, fu@mail.tuwien.ac.at

^bInstitute of Photogrammetry and Cartography, Technische Universitaet Muenchen, Arcisstr.21, 80333 Munich, Germany, {fan, stilla}@bv.tum.de

^cInstitute of Navigation, University of Stuttgart, Breitscheidstr.2, 70174 Stuttgart, Germany, wehr@nav.uni-stuttgart.de

Commission III, WG III/1

KEY WORDS: calibration, terrestrial laser scanner, ray tracing, Accuracy, coordinate system, adjustment.

ABSTRACT:

Within this paper an approach of calibration for a terrestrial laser scanner with two mirrors driven by two galvanometers is presented. This includes a mathematical model for the interior of the laser scanner as well as the determination for the parameters to be calibrated. The mathematical model is derived from the functionality of the laser scanner, whereby the principle of "Ray Tracing" was used. According to the inner structure of the scanner device and the functionality of the scanning system the laser ray would be divided into three parts. Every part could be represented by a metric length and a unit vector which could be deduced by using the algorithm in triangular angles and the matrix of reflection respectively. The mathematical model is then the result of combination of these three vectors of laser parts. It was suspected that the lengths of the laser ray and the angles of the mirror rotations were obtained inexactly during measurement. However they could be corrected by adding offsets and factors for the scale caused by not exact orthogonal configuration of the mirror axes. In order to estimate these parameters the adjustment model was established using the Gauss-Markov-Model. Results from the test with simulated data showed that the mathematical model and the adjustment model were adequate to the presented approach.

1. INTRODUCTION

In recent years laser scanning has found wide-spread use for acquiring geometric information for applications in cultural heritage documentation, forestry, forensics, deformation measurements, etc. The success of this relative new technology can be attributed to his advantages: (i) 3D Laser scanning records full automatically dense points clouds from the object surfaces with less effort than other 3D acquisition techniques; (ii) 3D Laser scanning is an active measuring system which allows the measurement independently of both the texture of the target object surface and the natural light conditions. For these reasons Laser scanning is becoming more and more popular nowadays. But most of available Laser scanners on the market are concerning the accuracy to the millimeter range. One of the important reasons is the lack of exact calibration for the opto-mechanical deflection of the Laser scanning mirror axes.

In the presented approach an experimental terrestrial laser scanner with two mirrors driven by two galvanometers was built up. Experiments have shown that the accuracy of this laser scanner in range is better than 2 mm. Although a very high precise opto-mechanical deflector for the two mirrors is used. For obtaining accurate 3D coordinates of the objects an additional scanner calibration is still required.

For measuring one point on the object surface, three observations are made, namely the range l , the angles γ_1 of the mirror on the horizontal axis, and the angle γ_2 of the mirror on the vertical axis. Normally, point clouds are processed in a Cartesian coordinate system which has to be converted from the spherical coordinate system. In our work we used a mathematical model for the scanning system, in which additional parameters were introduced. This model considers the inner structure of the laser scanner.

This model is based on the principle of "ray tracing". The laser ray could be divided into three parts: (i) in the first part the laser light runs from the laser centre to the middle of the first mirror, it would be represented by l_1 , (ii) the laser light is mirror reflected on the first mirror surface with a certain rotation angle γ_1 , then it runs to the second mirror. This part is the second part of laser ray, and would be represented with l_2 , (iii) the laser light is reflected on the second mirror surface with a rotation angle γ_2 and runs to the target object, this is the third part of the laser ray l_3 . Thus the propagate path results in five parameters, which consist of three distances l_1, l_2 and l_3 and two rotation angles γ_1 and γ_2 .

* Corresponding author. fan@bv.tum.de; phone +49 89 289-22586; fax +49 89 280-9573; www.carto-tum.de.

In the presented approach we assumed that the length of the first part of the laser light l_1 is known and constant and both of the angles between the optical axis and the laser path from the laser centre are zero. It was suspected, that the distances l_2 and l_3 were not exactly measured and the angles of the mirrors rotation γ_1 and γ_2 were incorrect, too. These four parameters should be corrected by the calibration, i.e.: 4 offsets $(dl_2, dl_3, d\gamma_1, d\gamma_2)$ to these four parameters $(l_2, l_3, \gamma_1, \gamma_2)$ should be found out by the calibration. Additionally to these offsets we introduced the parameters $m_{l_2}, m_{l_3}, m_{\gamma_1}$ and m_{γ_2} for the scale because of effects given by different Field of Views (FOV).

In order to estimate the eight parameters $(dl_2, dl_3, d\gamma_1, d\gamma_2, m_{l_2}, m_{l_3}, m_{\gamma_1}, m_{\gamma_2})$ the equations in the mathematical model were linearized. Then the adjustment model was established using the Gauss-Markov-Model. In the next step we simulated sets of measured data according to the functionality of the laser scanner. The data sets differ in FOV (16 degree and 19 degree). The simulated data were exploited to estimate the eight parameters and to validate the adjustment model. The results showed that the process of the adjustment is adequate to the presented approach.

The remainder of this paper is structured as follows: in the second section it will be described how the laser scanner works. According to this functionality the mathematical model is developed in the section three. In the fourth section the parameters to be calibrated will be introduced and the fifth section presents the test with simulated data. Finally, the conclusions are presented in the section six.

2. FUNCTIONALITY OF LASER SCANNER

The terrestrial laser scanner used in this work was built up at the Institute of Navigation, University of Stuttgart, Germany. The figure below shows the inner structure of this device.

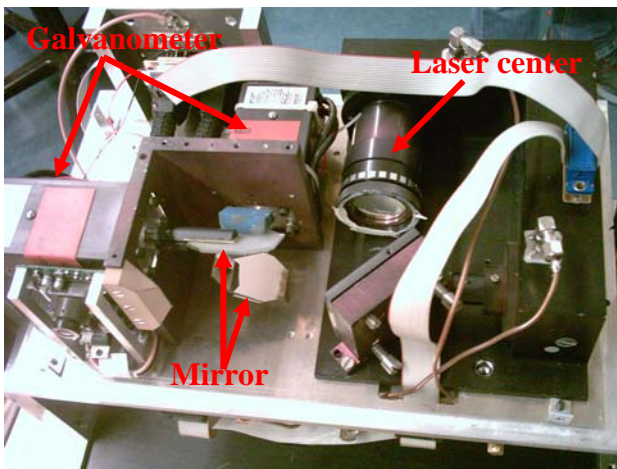


Figure 1. laser scanner with two galvanometers

Figure 1 shows the device without cage. And it can be abstracted as that shown in the figure 2. The main constituents

of the laser scanner are two rotation mirrors and laser centre, in which the laser beam could be emitted and received. The two mirrors are attached to rotor shafts of electric motors which have rotor capable of performing a limited rotation. The scanner device has also a position sensor of electrostatic capacitance type arranged around the rotor shaft of the motor, and output from this sensor is fed back to the instruction signal given to the motor, thereby to position the mirror. And the positions of the mirrors are given in angles. In the range measurement the CW-laser principle is applied which obtains the range by means of measuring the phase difference between the transmitted and the received signal backscattered from the object surface.

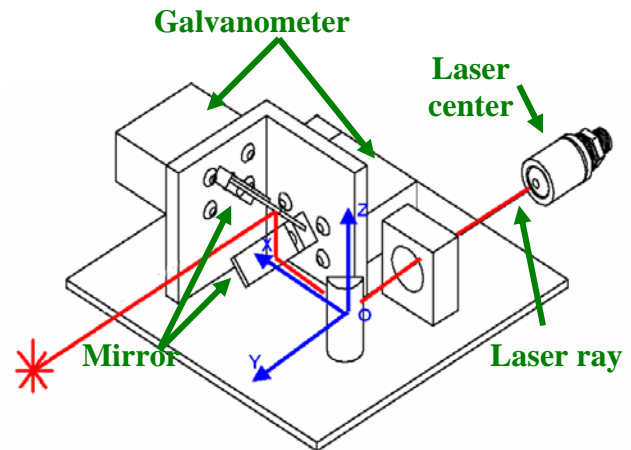


Figure 2. abstracted model of laser scanner. The red line represents the laser ray. The coordinate system (in blue) is the default coordinate system in the local scanning system.

The abstracted model shows the path of the laser ray clearly. At first laser light is emitted from the laser center. Then it runs to the first mirror. There it is reflected with a certain rotation angle of the mirror. Shortly after that it is reflected by the second mirror with another rotation angle. Finally, it runs to the target and then back to the laser center in the same way.

The technical data of this laser scanner can be cited in a table. Table 1. Technical data of the laser scanner in the presented work.

Laser output power:	0.5 mW
Laser wavelength:	670 nm
Instantaneous Field of View (IFOV):	0.1° (aperture by sending: 1 mm)
Field of View (FOV), variable:	Max. 30° x 30°
Aperture by receiving	24 mm
Sampling:	2-dim. Line scanning
Number of pixels per image:	200 x 200 or 400 x 400 (default setting)
Ambiguity interval:	> 10 m
Resolution Range:	0.1 mm (for diffuse reflectivity 60% and 1 m range)
Tone of measurement	10 MHz and 314 MHz
Measurement rate	2 KHz (working with one tone) 600 Hz (working with two tone)
Scanning rate	40 sec/scan

As shown in the first and second figures the terrestrial laser scanner requires distraction mechanisms in two different directions for surveying a certain region of an object of investigation, whereas the two mirrors were driven by two

galvanometers. A laser scanner of this type is also called a XY-Scanner. (Figure 3.)

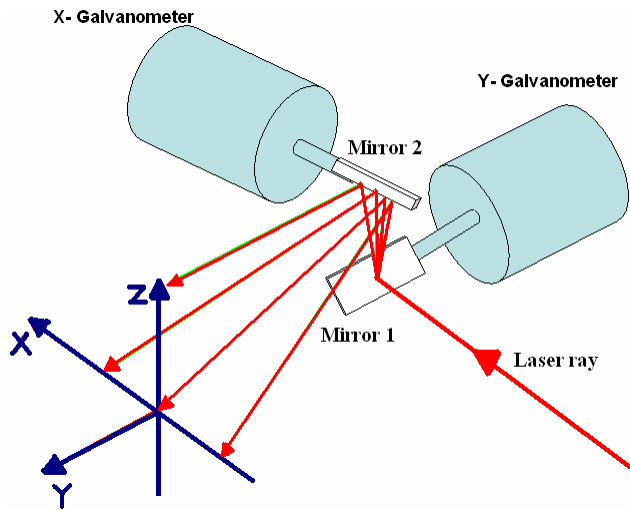


Figure 3. XY-Scanner

The figure 3 denotes the basic principle of the XY-Scanner. The two galvanometers should be installed orthogonally. The laser beam is initially reflected by the mirror driven by Y-Galvanometer. Afterwards, it is reflected by the mirror driven by X-Galvanometer.

For measuring one point on the object surface, three observations are made, namely the range l , the angles γ_1 of the mirror on the horizontal axis, and the angle γ_2 of the mirror on the vertical axis. Normally, point clouds are processed in a Cartesian coordinate system which has to be converted from the spherical coordinate system. In the presented work we established a mathematical model for the scanning system, in which additional parameters were introduced. This model considers the inner structure of the laser scanner which was described as the functionality of laser scanners in this section.

3. MATHEMATICAL MODEL

The mathematical model presented in this paper is established according to the principle of “ray tracing”. This including the involved coordinate systems and vectors of laser ray will be described in this section.

3.1 Coordinate systems and vectors

The mathematical model is based on the principle of “ray tracing”. The laser ray could be divided into three parts: (i) the first part l_1 represents the laser light running from the laser centre to the middle of the first mirror; (ii) the second part l_2 represents the laser light between the two mirrors (it is reflected on the first mirror surface with a certain rotation angle γ_1 , then it runs to the second mirror); (iii) the third part l_3 represents the laser light between the second mirror and the target (it is reflected on the second mirror surface with a rotation angle γ_2 and runs to the target object). Thus the propagate path results in

five parameters, which consist of three distances l_1, l_2 and l_3 and two rotation angles γ_1 and γ_2 .

In the presented approach we regarded these three parts of laser path as vectors. In order to describe these vectors detailed and obviously, it is necessary to introduce three coordinate systems, in which the three vectors lay respectively. (See. Table 2.)

Table 2. Coordinate systems in mathematical model

Coordinate system	Origin	X-axis	Y-axis	Z-axis
Origin coordinate system (N-system)	Laser centre point O	Parallel to the driving axis of the second mirror	Parallel to the driving axis of the first mirror	Perpendicular to his XY-plan
1. mirror coordinate system (S1-system)	Centre of the first mirror O'	Perpendicular ar to his Y-axis on the mirror plan	the driving axis of the first mirror	Perpendicular to the first mirror plan
2. mirror coordinate system (S2-system)	Centre of the second mirror O''	the driving axis of the second mirror	Perpendicular to his X-axis on the mirror plan	Perpendicular to the second mirror plan

Note: all of the three coordinate systems are right hand system.

The coordinate systems including the vectors of the three parts of the laser path could be illustrated in the graphic below. (Figure. 4)

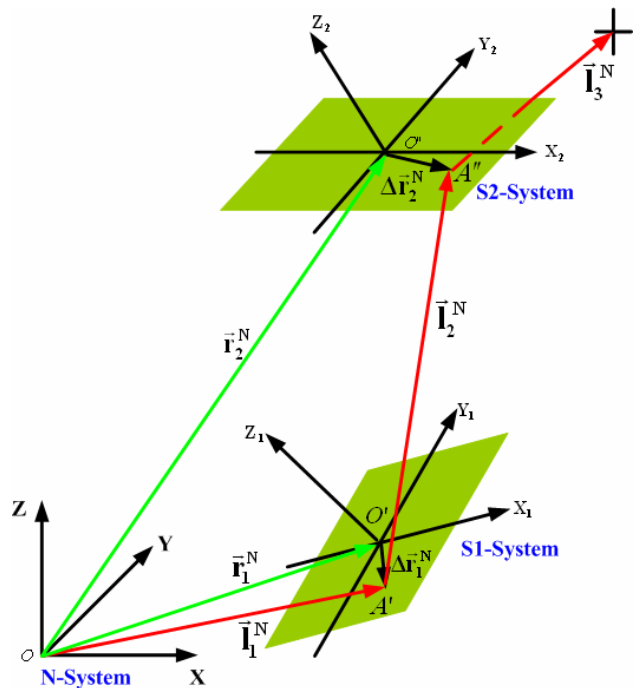


Figure 4. coordinate systems and vectors of the laser path

In the figure 4 A' is the incidence of the laser light on the first mirror and A'' represents the incidence of the laser light on the second mirror.

In different coordinate systems the vectors should be represented differently, as you can see in the table below.

Table 3. Explaining for vectors

vector		explaining
In N-system	In mirror coordinate system	
\vec{r}_1^N	\vec{r}_1^{S1} (in S1-system)	Vector to the centre of the first mirror (from O to O')
\vec{r}_2^N	\vec{r}_2^{S2} (in S2-system)	Vector to the centre of the second mirror (from O to O'')
\vec{l}_1^N	\vec{l}_1^{S1} (in S1-system)	The first part of laser vector (from O to A')
\vec{l}_2^N	\vec{l}_2^{S1} (in S1-system)	The second part of laser vector (from A' to A'')
	\vec{l}_2^{S2} (in S2-system)	
\vec{l}_3^N	\vec{l}_3^{S2} (in S2-system)	The third part of laser vector (from A'' to object)
$\Delta\vec{r}_1^N$	$\Delta\vec{r}_1^{S1}$ (in S1-system)	Vector from O' to A'
$\Delta\vec{r}_2^N$	$\Delta\vec{r}_2^{S2}$ (in S2-system)	Vector from O'' to A''

3.2 Rotation matrices

For the mathematical model two types of rotation matrices were needed. They would be defined and described in the following.

3.2.1 Matrix for reflection

According to the law of the reflection the laser ray is reflected at the mirror plan. Because the incident laser vector and the reflected laser vector have opposite directions in norm direction of the mirror plan, the matrix for reflection is then:

$$\mathbf{S} = \begin{pmatrix} 1 & 0 & 0 \\ 0 & 1 & 0 \\ 0 & 0 & -1 \end{pmatrix} \quad (1)$$

3.2.2 Rotation matrices for mirror coordinate systems

Using the rotation matrices the vectors can be transformed from the N-system to the mirror system (S1- or S2-system). In photogrammetry (Kraus 2004) the rotation and orientation of the mirrors could be described by dint of affine transformations.

$$\mathbf{R}_N^S = \mathbf{R}_x \cdot \mathbf{R}_y \cdot \mathbf{R}_z \quad (2)$$

Where \mathbf{R}_N^{S1} is the rotation matrix for the first mirror (S1-system) with the rotation angle γ_1 of the mirror on the horizontal axis, and \mathbf{R}_N^{S2} is the rotation matrix for the second mirror (S2-system) with the rotation angle γ_2 of the mirror on the vertical axis.

3.3 The known vectors

Aiming to simply the situation to a certain extent we assumed in the presented approach that both of the angles between the optical axis and the laser path from the laser centre are zero. On the other hand we got some known parameters for the device from manufacture as following:

- The distance between the laser centre and the centre of the first mirror is 0.0625 m.
- The distance between two mirrors is 0.036 m.

Then we have:

$$\vec{r}_1^N = \begin{pmatrix} r_{1x}^N \\ r_{1y}^N \\ r_{1z}^N \end{pmatrix} = \begin{pmatrix} 0.0625 \\ 0 \\ 0 \end{pmatrix} \quad (3)$$

and

$$\vec{r}_2^N = \begin{pmatrix} r_{2x}^N \\ r_{2y}^N \\ r_{2z}^N \end{pmatrix} = \begin{pmatrix} 0.0625 \\ 0 \\ 0.036 \end{pmatrix} \quad (4)$$

and the unit vector for the first part of the laser vector

$$\vec{u}_{l_1}^N = \begin{pmatrix} u_{l_{1x}}^N \\ u_{l_{1y}}^N \\ u_{l_{1z}}^N \end{pmatrix} = \begin{pmatrix} 1 \\ 0 \\ 0 \end{pmatrix} \quad (5)$$

3.4 The laser vectors

The first part of the laser vector was represented by convolution of the length of the first part of laser l_1 and its unit vector $\vec{u}_{l_1}^N$.

$$\vec{l}_1^N = l_1 \cdot \vec{u}_{l_1}^N \quad (6)$$

Under the assumption in section 3.3 vector \vec{r}_1^N is then the equivalence of the vector \vec{l}_1^N .

3.4.1 The second part of the laser vector

Analog to the equation 6 the second part of the laser vector could be calculated with the equation below:

$$\vec{l}_2^N = l_2 \cdot \vec{u}_{l_2}^N \quad (7)$$

where l_2 is the length of the second part of laser and $\vec{u}_{l_2}^N$ is its unit vector.

From the figure 4 we see that \vec{l}_2^N is the reflected vector of the incident vector \vec{l}_1^N , hence we can get $\vec{u}_{l_2}^N$ by using the matrix for reflection (equation 1). This process could be implemented in three steps:

- transform $\vec{u}_{l_1}^N$ from N-system to S1-system

$$\vec{u}_{l_1}^{S1} = \mathbf{R}_N^{S1} \cdot \vec{u}_{l_1}^N \quad (8)$$

(ii) use the matrix of reflection in S1-system

$$\bar{\mathbf{u}}_{l_2}^{S1} = \mathbf{S} \cdot \bar{\mathbf{u}}_{l_1}^{S1} \quad (9)$$

(iii) transform $\bar{\mathbf{u}}_{l_2}^{S1}$ from S1-system to N-system

$$\bar{\mathbf{u}}_{l_2}^N = (\mathbf{R}_N^{S1})^T \cdot \mathbf{S} \cdot \mathbf{R}_N^{S1} \cdot \bar{\mathbf{u}}_{l_1}^N \quad (10)$$

The calculation of the length l_2 was realized by disposing of triangle geometry:

(i) in the triangle $\Delta O''A'A''$ we have the equation

$$(\bar{\mathbf{r}}_2^{S2} - \bar{\mathbf{l}}_1^{S2}) + \Delta \bar{\mathbf{r}}_2^{S2} = \bar{\mathbf{l}}_2^{S2} \quad (11)$$

(ii) put equations 6 and 7 into 11 we can get

$$\mathbf{R}_N^{S2} \cdot (\bar{\mathbf{r}}_2^N - l_1 \cdot \bar{\mathbf{u}}_{l_1}^N) + \Delta \bar{\mathbf{r}}_2^{S2} = \mathbf{R}_N^{S2} \cdot l_2 \cdot \bar{\mathbf{u}}_{l_2}^N \quad (12)$$

The equation 12 is equivalent to the equation below:

$$l_2 = (\mathbf{R}_N^{S2})^T \cdot (\mathbf{R}_N^{S2} \cdot (\bar{\mathbf{r}}_2^N - l_1 \cdot \bar{\mathbf{u}}_{l_1}^N) + \Delta \bar{\mathbf{r}}_2^{S2}) \cdot (\bar{\mathbf{u}}_{l_2}^N)^{-1} \quad (13)$$

3.4.2 The third part of the laser vector

The third laser vector $\bar{\mathbf{l}}_3^N$ could be deduced in the same way as the second laser vector.

$$\bar{\mathbf{l}}_3^N = l_3 \cdot \bar{\mathbf{u}}_{l_3}^N \quad (14)$$

Since the third part of laser ray is the result of the mirror reflection of the second laser ray, the matrix of reflection would be used on the second mirror. Then the unit vector of the third part of laser could be derived:

$$\bar{\mathbf{u}}_{l_3}^N = (\mathbf{R}_N^{S2})^T \cdot \mathbf{S} \cdot \mathbf{R}_N^{S2} \cdot \bar{\mathbf{u}}_{l_2}^N \quad (15)$$

On the other hand, the length of the third part of laser was very simple to be calculated finally:

$$l_3 = l - l_1 - l_2 \quad (16)$$

where l is the total length of the laser from measurement.

Now the mathematical can be established by combining the three parts of laser vectors.

$$\begin{aligned} \begin{pmatrix} X \\ Y \\ Z \end{pmatrix} &= \bar{\mathbf{l}}_1^N + \bar{\mathbf{l}}_2^N + \bar{\mathbf{l}}_3^N \\ &= l_1 \cdot \bar{\mathbf{u}}_{l_1}^N + l_2 \cdot \bar{\mathbf{u}}_{l_2}^N + l_3 \cdot \bar{\mathbf{u}}_{l_3}^N \end{aligned} \quad (17)$$

4. PARAMETERS FOR CALIBRATION

It was suspected, that the distances l_2 and l_3 were not exactly measured and the angles of the mirrors rotation γ_1 and γ_2 were incorrect, too. These four parameters should be corrected by the calibration, i.e.: four offsets ($dl_2, dl_3, d\gamma_1, d\gamma_2$) to these four parameters ($l_2, l_3, \gamma_1, \gamma_2$) should be found out by the calibration. Additionally to these offsets we introduced the parameters $m_{l_2}, m_{l_3}, m_{\gamma_1}$ and m_{γ_2} for the scale because of effects given by different Field of Views (FOV).

In order to estimate the eight parameters ($dl_2, dl_3, d\gamma_1, d\gamma_2, m_{l_2}, m_{l_3}, m_{\gamma_1}, m_{\gamma_2}$) the equations (equ.17.) of the mathematical model were linearized. Then the adjustment model was established using the Gauss-Markov-Model.

5. TEST OF THE MATHEMATICAL MODEL AND THE ADJUSTMENT MODEL

In this section the mathematical model and the adjustment model would be tested by using simulated measurement data. For this proposal a set of measurement data was simulated in Cartesian according the functionality of the laser scanner (section 2). They were then transferred in angles and distances by using:

$$\begin{pmatrix} \gamma_1 \\ \gamma_2 \\ l \end{pmatrix} = \begin{pmatrix} (\arctan \left(\frac{X}{\sqrt{Y^2 + Z^2}} \right)) / 2 \\ (\arctan \left(\frac{Z}{Y} \right)) / 2 \\ \sqrt{X^2 + Y^2 + Z^2} \end{pmatrix} \quad (18)$$

In order to test the sensitivity of the mathematical model and the adjustment model we added known offsets and scale factors on the angles and the distances obtained by using equation 18. In figure 5 the two types of points are shown graphically, wherein the green points were the results of adding known offsets and scale factors on the simulated data (the red ones). All of the simulated points lay on a plan and the distance between neighbour points is three cm.

After the adjustment the same values as we had added were received for the parameter of the calibration, as shown in the figure 7, the green points (results after the adjustment) are almost identical with the red points (simulated data). This means that the mathematical model and the adjustment model are appropriate to the calibration and they are sensitive on the other hand.

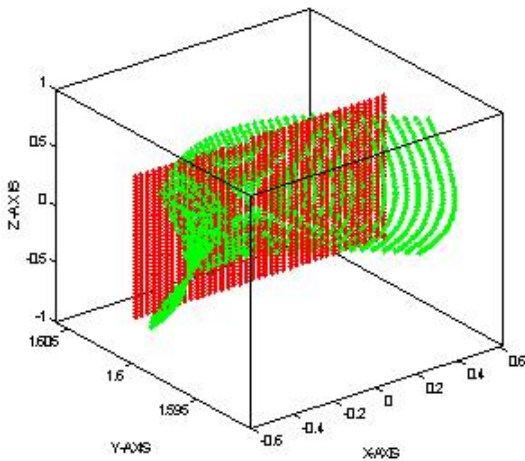


Figure 5. simulated data before adjustment. The green points were the results of adding known offsets and scale factors on the simulated data (the red ones).

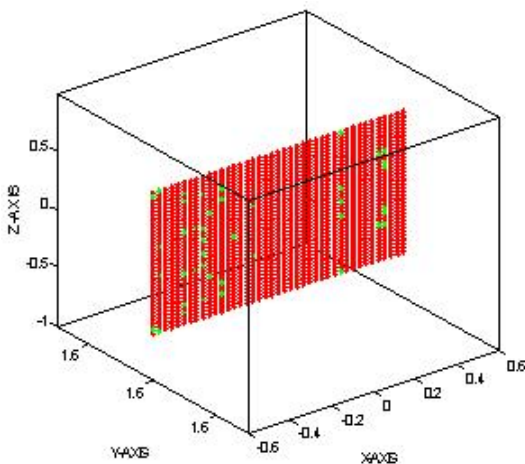


Figure 6. Data after adjustment in simulation

After the test for sensitivity using simulated data, a small white board was measured. The board was located vertically to the Y axis of the N-System. And the distance between the board and the XZ-plane of the N-System was around 1.6 meters. The measurement lasted around 30 minutes. And then the data and the known technical parameters of the device were stored in a text file. Due to the limitation that we did not have measure instrument with higher accuracy, control points for the calibration were not available. In this case we choose several points in the middle of the measurement field to fit a plan. The points on this fitted plan were viewed as the control points of the measured points respectively. Figure 7 presents the measured points with green color and the fitted plan with red color.

The result of the adjustment is shown in the figure 8. Comparing the green points between the measured data and the data corrected by adjustment it would be found that (i) the curvature of the original data was eliminated; (ii) the average distance between the corrected data and the fitted plan were significantly smaller than that before adjustment; and (iii) the points after the adjustment had a normal contribute. These could mean that the adjustment is able to correct the measured data in great extent.

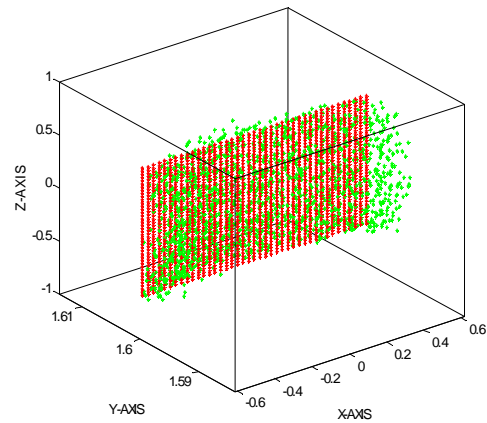


Figure 7. Measured data (in green) and their approximated plan (in red)

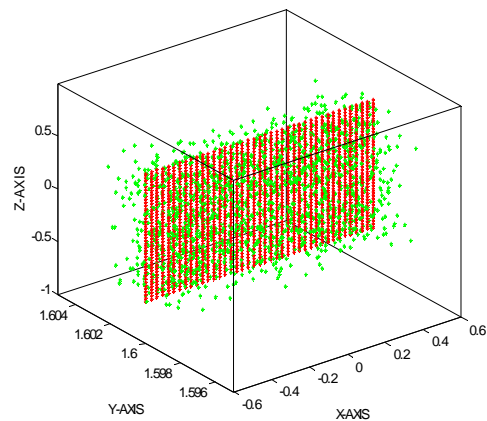


Figure 8. Results of the adjustment

6. CONCLUSION

This work presented a mathematical model for the laser scanner driven by two galvanometers according the principle of “ray tracing”. In the mathematical model the laser ray was treated as three parts of laser vectors represented by metric lengths and unit vectors. And they could be deduced respectively by using the algorithm in triangular angles and the matrix of reflection. Then the mathematical model is a combination of the three vectors. On the base of the mathematical model the parameters for calibration could be derived.

The simulation denoted that the developed model was sensitive. And the test showed that the adjustment model could correct the measured data in great extent, although there were not control points for the adjustment.

7. REFERENCES

- Kraus, K. 2004. *Photogrammetry*. Walter de Gruyter, Berlin. New York, pp. 5-16.
- Vozikis, G., Haring, A., Vozikis, E., Kraus, K., 2004, Laser Scanning: A New Method for Recording and Documentation in Archaeology, Paper ID WSA1.4
- Wehr, A., Thomas, M. 2006. Close range Laser scanner, Stuttgart, Germany. http://www.nav.uni-stuttgart.de/navigation/forschung/nahbereich_laserscanner/